International Journal of Nanoelectronics and Materials
Volume 16, No. 4, October 2023 [883-890]

The Enhancement Light Absorption of ZnO-TiO_2 Nanocomposite as Photoanode

Muhammad Asnawir Nasution[1], Iwantono[1*], Puji Nurrahmawati[1], Nashiha Chalvi Syahra[1], Ari Sulistyo Rini[1], Suratun Nafisah[2], Romi Fadli Syahputra[3], Marlia Morsin[4]

[1]Department of Physics, Universitas Riau, 28293 Simpang Baru, Riau, Indonesia
[2]Department of Electrical Engineering, Institut Teknologi Sumatera (ITERA), 35365 Way Hui, Lampung Selatan, Indonesia
[3]Department of Physics, Universitas Muhammadiyah Riau, Riau, Indonesia
[4]Microelectronic and Nanotechnology – Shamsuddin Research Centre (MiNT-SRC), Institute of Integrated Engineering, Universiti Tun Hussein Onn Malaysia, 86400 Parit Raja, Batu Pahat, Malaysia

Received 26 October 2022, Revised 20 January 2023, Accepted 7 February 2023

ABSTRACT

ZnO nanomaterial in Dye Sensitized Solar cells (DSSC) has the disadvantage of low efficiency. The purpose of this study was to improve the DSSC efficiency of the ZnO photoanode. ZnO-TiO_2 nanocomposites are used as photoanodes that can improve light absorption. ZnO-TiO_2 nanocomposites can increase the performance efficiency of the solar cell compared to ZnO Pristine. This is due to the reduced recombination between ZnO/electrolyte and the increased lifetime of electrons because of the presence of electrons trapped in TiO_2. The most optimal sample from this study was found in ZnO-TiO_2 nanocomposite with a volume concentration ratio (85%-15%) because the efficiency DSSC increases almost 2 times.

Keywords: Absorption, DSSC, Photoanode, TiO_2, ZnO

1. INTRODUCTION

DSSC is the third generation of solar cells. DSSC is still being developed because the theoretical efficiency of solar cells can reach 86.6% with a multi-junction design [1]. However, DSSC still has its drawbacks, namely low absorption, unstable electrolytes, and low efficiency [2]. So, it is necessary to make improvements to get an efficient DSSC.

Modification of DSSC in increasing sensitivity so that light absorption increases can be done by doping [3], modification of nanostructure [4-5], and using scattering materials [6]. Modification of the scattering material can be done effectively by blocking layer design, modification of one-dimensional nanostructure, and generation of high scattering effect [4].

This study proposes a reflective layer made by nanocomposites for enhancing optical absorption and charge carriers. Nanocomposites are a combination of two or more materials to obtain better properties. The results of the ZnO/TiO_2 nanocomposite research can increase electron transport 100 times faster than TiO_2 [7]. The properties and photovoltaic performance of the proposed nanocomposites are provided.

* Corresponding author: iwantono@lectuere.unri.ac.id

2. MATERIAL AND METHODS

2.1 Sample Preparation

The ZnO nanorods on glass substrates were prepared using seed mediated and hydrothermal methods. The ZnO seed layer was deposited on FTO via drop technique until fully covered using 0.1 M zinc acetate dihydrate (ZAD). The seeding was heated at 100 °C for 15 min. The layer of seeding was done 3 times. The seeding was annealed at 350 °C for 1 h on a hot plate and then cooled down to room temperature. After the seeding process, the samples were soaked in a growth solution by hydrothermal method [8].

The growth solution was mixed with 0.1 M of zinc nitrate hexahydrate (ZNH) and hexamethylenetetramine (HMT), adding TiO_2 as a composite from titanium tetra isopropoxide (TTIP). The concentration volume variations of nanocomposite ZnO-TiO_2 which is given in Table 1 are proposed to obtain the best performance sample. The seeding was placed in the growth solutions at an angle of 45° to the horizontal plane for 8 h at 90 °C in an oven. The samples were then taken out and washed several times using distilled water in order to remove any precipitation and then the samples were dried.

Table 1 Concentration of ZnO and TiO_2 precursor for each sample.

Sample	ZnO (%)	TiO_2 (%)
A	75	25
B	80	20
C	85	15
D	90	10
E	100	-

2.2 Characterization

The optical properties using wavelength 200-800 nm for the samples were measured by spectrophotometer UV-1800 Shimadzu. The crystal structure of samples was determined by powder X-ray diffraction (XRD) using an X'Pert powder (40 kV,30 mA) with Cu Ka radiation λ= 0.154 nm). The diffraction patterns were scanned from a diffraction angle (2θ) 20° to 80°. The sample's morphology was analyzed using a Jeol JSM-7600F scanning electron microscope (SEM). The performance of DSSC was analyzed using Keithly 2430 SourceMeter.

3. RESULTS AND DISCUSSION

3.1 Optical Properties

The absorption spectrum of ZnO with varying volumes of TiO2 using the hydrothermal method is shown in Figure 1. The absorption spectrum was taken in the wavelength range of 350-800 nm. Based on Figure 1 the strong absorption occurs at a wavelength of 350-375 nm. The characteristics of the UV-Vis absorption spectrum for ZnO nanorods with strong absorption are at a wavelength of 200-400 nm [9]. The spectrum absorbance showed an increase in the absorption of the samples E-C (the addition of TiO_2 up to 15%) and the samples C-A (TiO_2 was added more than 15%) decreased in the absorption. The highest absorption was found in sample C and the lowest absorption was in sample E (ZnO pristine). The addition of TiO_2 to ZnO can increase the absorption of light as seen in Figure 1. This is due to a shift towards longer

wavelengths (redshift) [10]. It is indicated that more free electron has been formed. So that, the addition can improve light absorption.

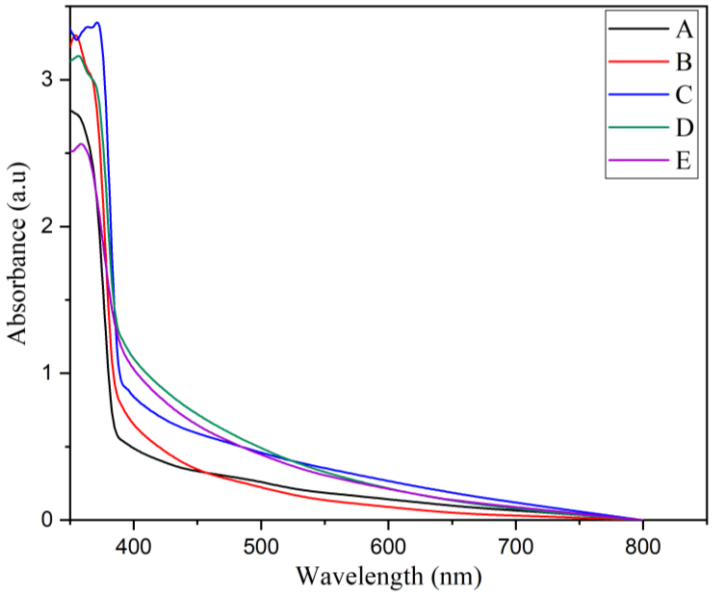

Figure 1. Absorbance spectrum of the samples.

Figure 2 shows the band gap energy of the sample. The band gap energy of the ZnO nanorod is around 3.17 eV- 3.24 eV [11]. The result of the sample can be seen in Table 2. The band gap energy in sample B-D shows a greater increase compared to sample A. It can be explained by the quantum confinement effect. That is, the energy value of the bandgap and the crystallite size are inversely proportional, meaning that the larger the crystallite size, the smaller the bandgap [12].

Table 2 The result of the energy bandgap

Sample	Energy gap (eV)	Absorbance (a.u)
A	3.24	2.75
B	3.26	3.16
C	3.20	3.39
D	3.21	3.29
E	3.18	2.57

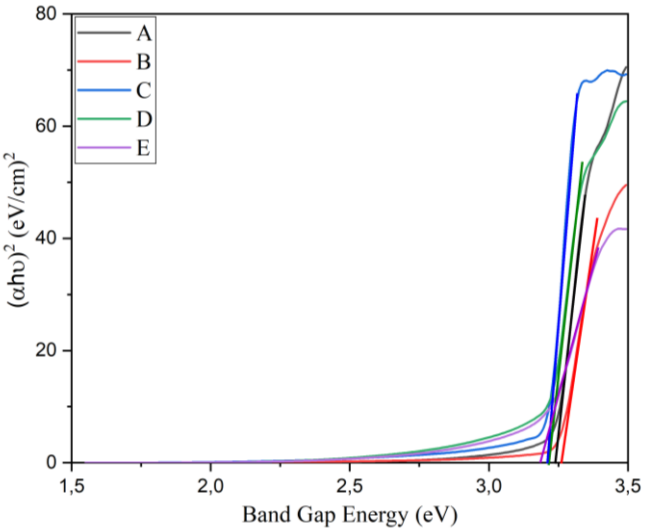

Figure 2. The band gap energy of the samples

3.2 Structural Properties

The XRD characterization is used for analyzing crystal structure from samples and it can be seen in Figure 3. It is indicated each element or compound has a different diffraction structure. It can be observed that ten peaks of diffraction at 2θ angles are 31,71°, 34,41°, 36,25°, 47,53°, 56,60°, 62,82°, 67,94°, 69,09°, 72,59°, and 76,96°. Diffraction patterns corresponding to the crystal plane are (010), (002), (011), (012), (110), (013), (112), (021), (004), and (022). The diffraction peaks and lattice were followed by ICSD No. 98-018-0052 for ZnO. The crystal structure of ZnO is hexagonal and it has lattice parameters of a =b 3,2530 Å and c = 5,2080 Å. Meanwhile based on ICSD No. 98-015-4036 TiO_2 are formed in peaks at 2θ angles 27,32°, 31,71°, 51,62°, 56,60°, 62,82°, and 72,59°. Half of TiO_2 peaks appear at the same time as ZnO which is considered the dominant ZnO peak because the percentage used is more ZnO dominant. TiO_2 peaks that do not overlap with ZnO are marked with an asterisk (*).

Table 3 shows of structural properties of the sample. The strongest line of all of the samples is at the (002) crystal plane. The crystalline size of samples C and E are the same (27.61 nm) but the position is slightly shifted. This is because of the difference in ionic radius between Zn+2 (0.75Å) and Ti^{+4} (0.61). So if more TiO_2 concentration is added, the angle will shift in a larger direction [13]. The results of sample A-D have shifted the angle from sample E.

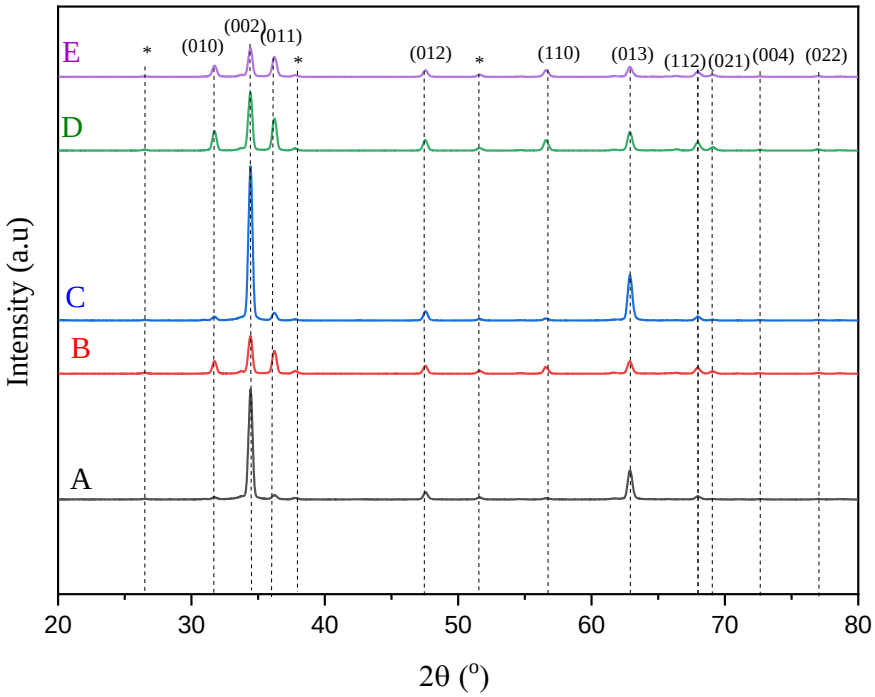

Figure 3. X-ray diffractogram of the samples.

Table 3 Structural properties of the samples

Sample	2θ	Crystalline Size (nm)	FWHM
A	34.48	23.25	0.374
B	34.47	22.64	0.384
C	34.44	27.61	0.315
D	34.42	18.11	0.480
E	34.38	27.61	0.315

3.3 Morphological Properties

The FESEM characterization is used to determine the morphology (shape and size) of a nanomaterial. The FESEM picture in Figure 4 shows the formation of ZnO and ZnO/TiO_2 nanorods. The diameter of the nanorods obtained for samples C and E were 80 nm and 210 nm respectively. The homogeneity of the ZnO nanorod in samples C and E looks more homogeneous than in sample A. The shape of samples C and E are fully formed and standing but there are different sizes. Sample A cannot be measured in diameter because the nanorod of ZnO/TiO formed has been damaged. So, it can be assumed that the presence of TiO_2 composite causes ZnO nanorods to be smaller until they are damaged. According to a study [14], ZnO/TiO_2 nanocomposites with ratios of 6%:94% and 20%:80% resulted in TiO_2 particles with similar shapes and smaller sizes due to the dispersion of ZnO aggregates. So, ZnO particles are incorporated into TiO_2. In this case, samples C and E can be explained by the formation of ZnO/TiO_2 composites. The dominant ZnO is similar to a ZnO nanoparticle, while agglomeration and smaller nanorod size in the composites are caused by dispersed TiO_2 aggregates that have entered into the ZnO. So, if the high TiO_2 percentage can be covered by ZnO nanorod by TiO_2 it can be seen in Figure A.

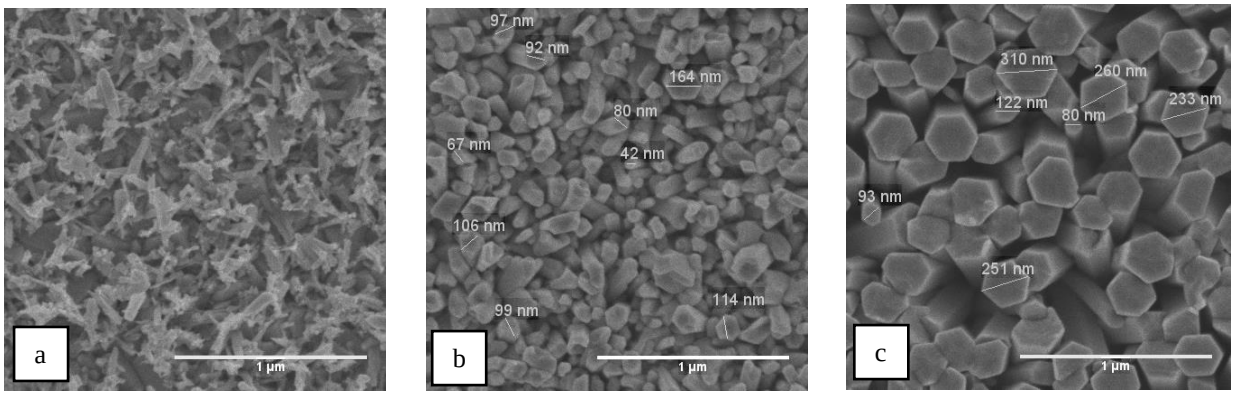

Figure 4. Morphology of the samples. SEM image of sample A (a), sample C (b), and sample E (c). All image is magnified by 20,000 times.

3.4 Photovoltaic Performance

The result of optical and morphology properties is increased absorption and the homogeneity of shape and size. Figure 5 illustrates the process of light absorption, which can increase efficiency by limiting charge recombination at the semiconductor/electrolyte interface.[15].

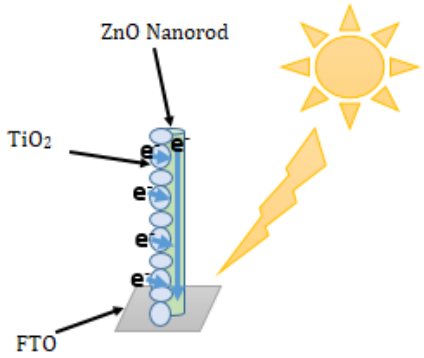

Figure 5. Scheme of light absorption.

The result of optical and structural band gap energy and crystalline size is in concert with the quantum confinement effect. The large crystallite size can enhance conductivity electrical because the atomic arrangement is regular. The large electron conductivity can increase the electrons distributed to the photoanode [16].

Figure 6 shows the results of the J-V characteristic of the sample. Based on Figure 6, it shows the broad to narrow areas, namely C, A, D, B, and E. The J-V characteristics are in line with the results of the UV-Vis, XRD, and SEM characterizations. The results of the J-V test show that the highest efficiency is found in samples C, A, D, B, and E. The results of the I-V test are shown in Table 4.

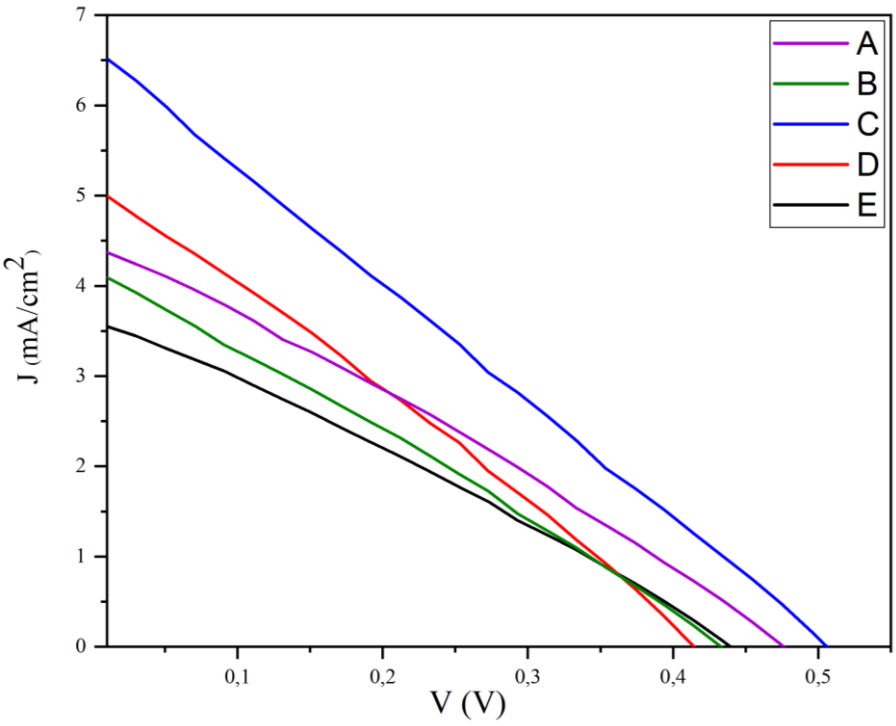

Figure 6. J-V characteristic solar device of the samples.

The current density generated (J_{sc}) from sample A-D is increased compared to sample E, this is because high light absorption will result in high electrical conversion. The absorption of light produced by ZnO/TiO_2 nanocomposite is greater than that of pure ZnO. Another reason, for the increased value of Jsc ZnO/TiO_2 is due to the increased electron lifetime of ZnO passivated on the TiO_2 surface, providing a better electron percolation path compared to ZnO-Photoanade [17]. In this study, the optimal results were found in sample C which achieved an efficiency of 87.8% compared to the pristine ZnO (sample E).

Table 4 The Optimized solar cell J-V characteristic of the photovoltaic parameter

Sample	Open circuit voltage, V_{oc} (V)	Photocurrent density, J_{sc} (mA/cm²)	Efficiency, η (%)	Fill factor (%)
A	0.475	4.21	0.604	28.45
B	0.434	4.09	0.498	28.04
C	0.515	6.47	0.845	24.02
D	0.414	5.11	0.584	26.87
E	0.455	3.60	0.450	27.16

4. CONCLUSION

The findings indicate that using ZnO-TiO_2 nanocomposite can enhance light absorption and J_{sc}, shifting the structure angle. Furthermore, increasing the concentration of TiO_2 in ZnO leads to smaller and more damaged ZnO nanorods. The nanocomposite C (85:15%) produces the highest efficiency and enhances 87.8% of the pristine ZnO sample.

ACKNOWLEDGEMENTS

This research work was funded by DRTPM Kemdikbudristek through LPPM Universitas Riau under the scheme of Magister Research Project (PTM) 2022 No. 1658/ UN19.5.1.3/ PT.01.03/2022. We also thank the Nanomaterial Laboratory-Department of Physics (Universitas Riau) and Universiti Tun Hussein Onn Malaysia (UTHM) for the facilities.

REFERENCES

[1] C.B. Honsberg, R. Corkish, S.P. Bremner, Proc. 17th Photovoltaic European Conference, Munich, (2001), 22-26.

[2] Sharma, K., Sharma, V. , Sharma, S.S., Nanoscale Res. Lett. 6, (2018) 1-46.

[3] Iwantono, I., Nurrahmawati, P., Natalia, S., Syahputra, R.F., Awitdrus, A. Zulkarnain, Z., Umar, A. A., Int. J. Nanoelectron. Mater. 13 (2020) 501–508.

[4] Sulaeman, U., Abdullah, A. Z., Renew. Sustain. Energy Rev. 74 (2017) 438–452.

[5] Albaihaqi. Y., Abdi, R., Natalia, S., Syahputra, R.F., Awitdrus, Iwantono, Key Eng. Mater. 860 (2020) 253–259.

[6] C. Rajkumar, A. Arulraj, Light scattering materials as photoanodes, in A. Pandikumar, K. Jothivenkatachalam, K. Bhojanaa, Interfacial Engineering in Functional Materials for Dye-Sensitized Solar Cells, John Wiley & Sons, Inc., United States, (2020) pp. 79-105.

[7] Manthina, V., Juan, P.C. Baena., Guangliang, L., Alexander. G., *J. Phys. Chem. C*, 116 (2012) 23864–23870.

[8] Asnawir, M., Iwantono, I., Anggelina, F., Awitdrus, Umar, A. A. Proc. of Seminar Nasional Fisika Universitas Riau, (2016) 104-111.

[9] Li, X., Chen, X., Yi, Z., Zhou, Z., Tang, Y., Yi, Y., Micromachines. 10 (2019) 1-13.

[10] Saima, N., Shamaila, S., Leghari, S. A. K., Shaheen, S., Iqbal, A., Mater. Res. Express. 27, (2018) 1-31.

[11] Sáenz-Trevizo, A., Amézaga-Madrid, P., Pizá-Ruiz, P., Antúnez-Flores, W., Miki-Yoshida, M., Mater. Res. 19 (2016) 33–38.

[12] Carol, T.T.T., Srivastava, A., Mohammed, J., Sharma, S., Mukhtar, G., Srivastava, A.K., SN Appl. Sci. 2 (2020) 1–8.

[13] Ali, M.M., Haque, M.J., Kabir, M.H., Kaiyum, M.A., Rahman, M.S., Results in Mater. 11 (2021) 100199(1-9).

[14] Ramírez-Ortega, D., Meléndez, A.M., Acevedo-Peña, P., González. I., Arroyo, R., Electrochim. Acta. 140 (2014) 541–549.

[15] Hernández, S. Cauda, V., Chiodoni, A., Dallorto, S., Sacco, A., Hidalgo, D., Celasco, E., Pirri C.F., ACS Appl. Mater. Interfaces. 6 (2014) 12153–12167.

[16] Wu, J., Chen, G.-R., Yang, H.-H., Ku C.-H., Ku, Lai, Jr.-Y., Appl. Phys. Lett., 90 (2007) 213109 1-213109 3.

[17] Hussein, A.M., Lefanova, A.V., Koodali, R.T., Logue, B.A., Energy Rep., 4 (2018) 56–64.